Electrochemical and Solid-State Letters, **12** (9) H336-H339 (2009)
1099-0062/2009/12(9)/H336/4/$25.00 © The Electrochemical Society

Solution-Processed, High Performance Aluminum Indium Oxide Thin-Film Transistors Fabricated at Low Temperature

Young Hwan Hwang, Jun Hyuck Jeon, Seok-Jun Seo, and Byeong-Soo Bae*,z

Department of Materials Science and Engineering, Laboratory of Optical Materials and Coating, Korea Advanced Institute of Science and Technology (KAIST), Daejeon 305-701, Korea

Thin-film transistors (TFTs) with aluminum indium oxide channel layers were fabricated via a simple and low cost solution process. The substitution of Al on In sites in the In_2O_3 lattice was verified by X-ray diffraction analysis. The maximum heat-treatment temperature of these transistors was 350°C, and the resultant thin films were highly transparent (with >90% transmittance). The fabricated TFTs operated in an enhancement mode on a positive bias and showed an n-type semiconductor behavior. They exhibited a channel mobility of 19.6 cm^2/V s, a subthreshold slope of 0.3 V/decade, and an on-to-off current ratio greater than 10^8.
 [DOI: 10.1149/1.3156830]

Manuscript submitted March 24, 2009; revised manuscript received May 27, 2009. Published June 25, 2009.

Metal-oxide-semiconductors have many advantages such as transparency due to their large bandgap, high uniformity in large-scale fabrication applications, environmental stability, and high electron conduction property.[1-4] Many transparent oxide semiconductors (TOSs), such as zinc- and indium-based oxide materials, have been reported for transparent channel layers in thin-film transistors (TFTs).[5-11] They exhibited mobilities and on-to-off current ratios in the range of 5–100 cm^2/V s and 10^6–10^7, respectively. Most TOSs, however, have been prepared by vacuum-deposition methods, such as radio-frequency-magnetron sputtering and pulsed laser deposition, which enable low temperature processes (even at room temperature) but require expensive equipments and result in high fabrication cost.

Solution-processed thin-film deposition techniques, such as spin coating, dip coating, and roll coating, offer many advantages over vacuum-deposition processes: simplicity, high throughput, and low cost.[12-14] They enable direct patterning that could replace conventional photolithographic techniques.[15-17] Recently, indium oxide and indium zinc oxide based TFTs have been fabricated by the solution process. The TFTs show a high mobility of 16 cm^2/V s and an ink-jet printability. However, most solution-processed TFTs require a high temperature annealing process usually over 500°C and have a high off-current and a low on-to-off current ratio of 10^6 compared to the typical vacuum-processed TFTs, which reduce the effective switching property.

Solution-processed oxide materials require an annealing process. Anion groups, which induce hysteresis and reduce electrical stability, are removed, and bonds between cation and oxygen are generated during annealing. Hence, a high annealing temperature is usually required to remove unnecessary anion groups. A high annealing temperature, however, limits the use of various substrates and restricts the applications. In this research, metallorganic precursors were used to decrease the annealing temperature rather than metal-chloride precursors, which are usually decomposed at higher temperatures than metallorganic precursors.[12,18,19]

We propose a multicomponent oxide, aluminum indium oxide (AIO), to fabricate the high performance TFT through the solution process. In_2O_3 has attracted a great deal of attention as a transparent conducting oxide and a semiconducting oxide due to the good electron transport property.[9,11] Hosono et al. reported that the overlapping of s orbitals of heavy-metal cations with $(n-1)d^{10}ns^0$ ($n \geq 4$) encourages high mobility even in the case of the amorphous phase.[8] Thus, metal cation species are the primary factors affecting the electron-transport property in TOSs, and use of a large cation such as indium is inevitable for high performance electrical devices.[20,21] Solution-processed In_2O_3 semiconductors by itself, however, could not achieve a sufficient low off-current and a high mobility simultaneously.[22] In this research, it was observed that the electrical property of TFTs was improved by substituting Al on In sites in the In_2O_3 lattice structure.

The metal precursor solution for the AIO channel layer was prepared by dissolving 0.04 M of aluminum acetylacetonate [$Al(C_5H_7O_2)_3$, Aldrich] and 0.1 M of indium acetate [$In(C_2H_3O_2)_3$, Aldrich] in 2-methoxyethanol [$C_3H_8O_2$, Aldrich]. To form a stable solution, the indium acetate precursor was chelated with 0.4 M of ethylenediamine ($NH_2CH_2CH_2NH_2$, Aldrich). The solution was stirred at room temperature for half an hour to make a transparent and homogeneous solution. The amount of aluminum in the final precursor solution was 40% of indium. After that, the solution was filtered through a 0.22 μm syringe filter [poly(tetrafluoroethylene), GE] and was spin coated at a speed of 5000 rpm atop the SiO_2/Si substrate for 30 s. Fifty W of oxygen plasma treatment was applied for 5 min just before spin coating to remove unnecessary organics on the substrate using a conventional plasma cleaner. A 100 nm SiO_2 layer, which served as a gate dielectric, was thermally grown on top of the heavily boron (p^+)-doped silicon wafer. After film deposition, it was annealed on a hot plate at 350°C for 2 h in air. The resultant annealed thin film contained ~10 atom % of aluminum compared to indium characterized by the transmission electron microscopy (TEM)–energy-dispersive spectroscopy measurement due to the volatilization of aluminum acetylacetonate during spin coating and annealing.

Thermogravimetric analysis (TGA) of the AIO precursor solution shows that thermal decomposition is completed before 350°C is reached (Fig. 1a). The TGA indicates that 350°C is enough annealing temperature to remove unnecessary organics in the film. The maximum heat-treatment temperature of 350°C, which is still relatively low compared to those of other solution-processed metal oxide TFTs (usually over 500°C),[18,23] could allow for the use of low cost substrates, such as soda-lime glass and plastic films, rather than the high cost substrates commonly used for transparent electronics. The initial weight loss below 150°C was due to the evaporation of the residual solvent (i.e., 2-methoxyethanol). The aluminum acetylacetonate began to decompose at ~160°C, and its decomposition was completed at ~230°C. The abrupt weight loss at around 270–330°C was attributed to the decomposition of indium acetate.

The decisive effect of aluminum is apparent in the X-ray diffraction (XRD) patterns of In_2O_3 and AIO films shown in Fig. 1b. It is observed that the peak of AIO, which appears at 30.71°, is shifted to a higher angle by 0.13° compared to (222) of an In_2O_3 crystal, which is shown at 30.58°. The shift in peak implies two important features. First, aluminum and indium ions form multicomponent composites rather than exist separately. Second, a shift to a higher angle indicates that the lattice constant is decreased. Because the ionic radius of Al^{3+} is smaller than that of In^{3+}, the substitution of Al on In sites in the In_2O_3 lattice could lead to a shrinkage of the lattice

* Electrochemical Society Active Member.
z E-mail: bsbae@kaist.ac.kr

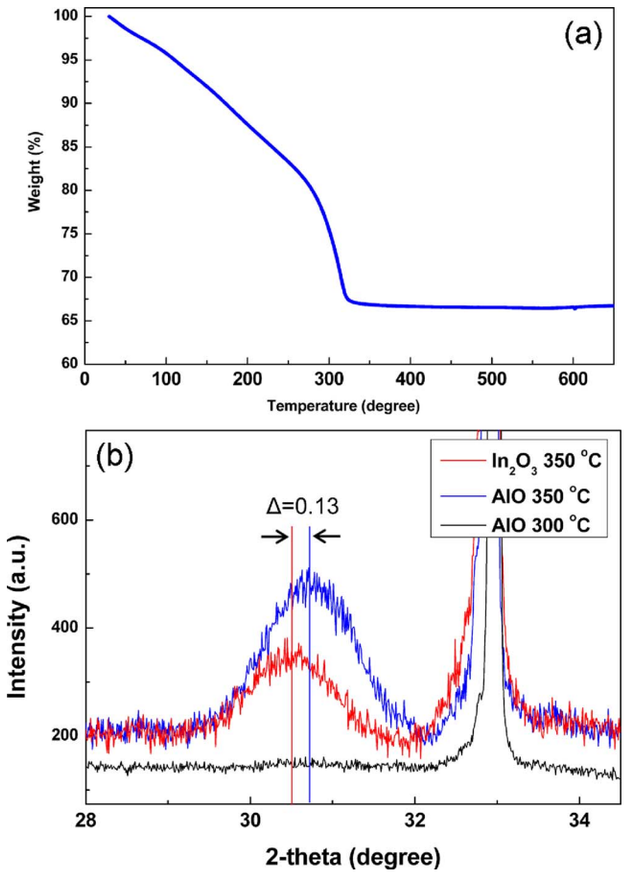

Figure 1. (Color online) (a) TGA of AlO precursor solution under air at a heating rate of 5°C/min. (b) θ-2θ XRD analysis of AlO films annealed at 300°C for 4 h and at 350°C for 2 h and that of In_2O_3 film annealed at 350°C for 2 h on SiO_2/Si substrate.

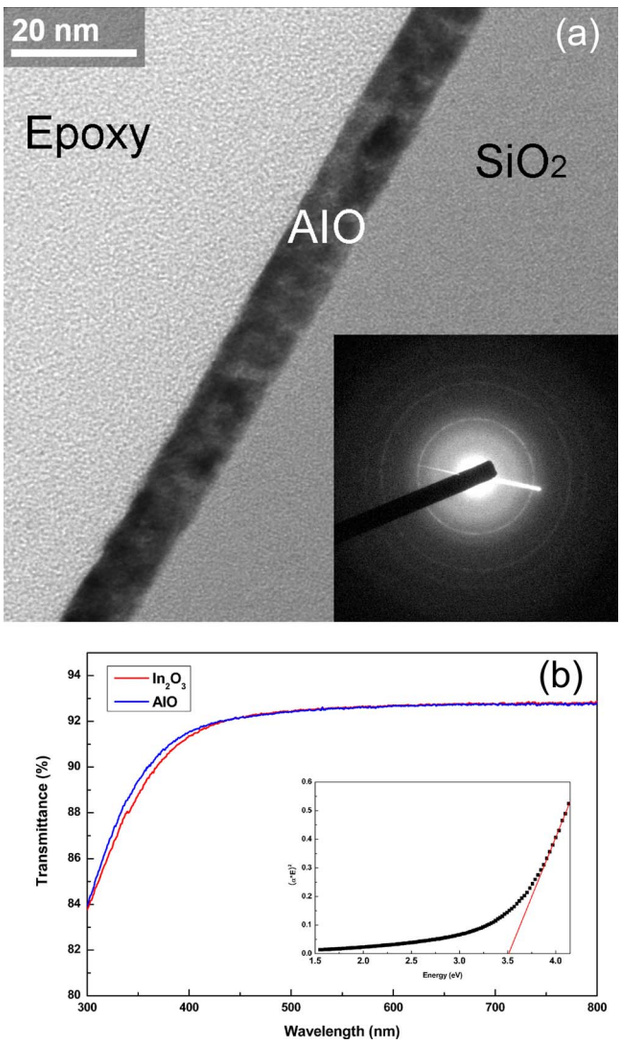

Figure 2. (Color online) (a) Cross-sectional TEM image and DP (inset) of AlO thin film annealed at 350°C for 2 h on SiO_2/Si substrate. (b) Transmittance spectra of AlO (blue line) and In_2O_3 (red line) thin films annealed at 350°C for 2 h deposited on quartz substrate and bandgap estimation of AlO thin film (inset).

and would be related to the reduction in the lattice constant.[24] Furthermore, the broadened peak suggests that substitution of Al creates more defect sites. Figure 2a and its inset present the cross-sectional TEM image and the diffraction pattern (DP) of the AlO thin film, respectively. The thickness is about 10 nm, and the morphology is uniform. A nearly discrete halo pattern is observed in the DP. The pattern indicates that the film is in the transition state from the amorphous phase, which is dominant in this film, to the crystalline phase.

The optical transmittance was measured at 300–800 nm wavelengths. The transmission spectrum of the AlO thin film indicates that it is optically transparent; more than 90% transmittance in most of the visible-light region was observed (Fig. 2b). The optical absorption coefficient, which was calculated from the transmittance, was used to determine the optical bandgap. The resultant bandgap of AlO is ~3.5 eV (inset of Fig. 2b), while In_2O_3 fabricated by the same procedure is ~3.4 eV. The shift in transmission spectra, which originates from the enlarged band structure, also supports the composite structure consisting of Al and In.[24]

After the fabrication of TFTs, the performances of the devices were measured in a dark room under ambient atmosphere using an HP 4145B semiconductor parameter analyzer. The AlO TFTs show a sufficient electrical property to drive display devices with the 100 nm SiO_2 gate dielectric layer, which can be easily deposited by various methods and can be widely used. The structure used for characterizing the fabricated TFTs was bottom-gate, top-contact type. 100 nm of aluminum source and drain electrodes were deposited by an E-beam evaporator through a shadow mask under a pressure of ~10^{-6} Torr. The fabricated channel length and width were 220 and 1000 μm, respectively. Figure 3a shows the drain current vs drain-to-source voltage (I_D-V_{DS}) output characteristics of the AlO TFT for various gate voltages (V_G). Transfer characteristic, I_D and $I_D^{1/2}$ vs V_G at a fixed V_{DS} = 40 V, is also displayed in Fig. 3b. Because clear pinch-off and current saturation behaviors were observed in the output characteristics, it seems reasonable to adopt the standard TFT theory to explain the operation of the AlO TFTs.[8] In terms of quantifying the performance of the semiconductor channel layer, specifically in terms of current driving capability and switching frequency, the most important TFT electrical property is channel mobility. The channel mobility and the threshold voltage were derived from linear fits to the dependence of the square root of I_D on V_G using the following equation in the saturation region

$$I_D = \frac{WC_i}{2L}\mu(V_G - V_{th})^2$$

Here, W, L, μ, C_i, and V_{th} are the channel width, channel length, channel mobility, capacitance per unit area of the SiO_2 gate insulator (dielectric constant ~3.9), and threshold voltage, respectively. The

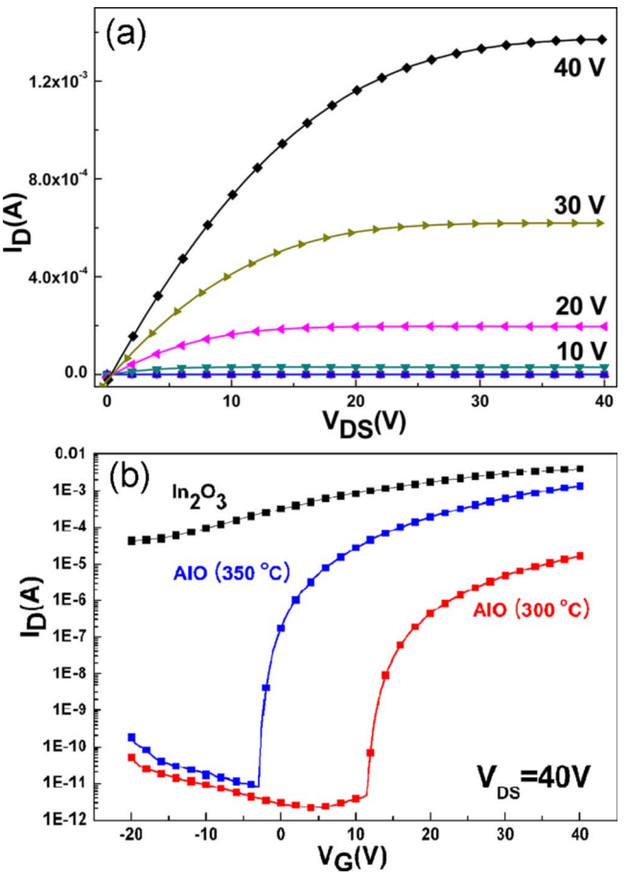

Figure 3. (Color online) (a) Output characteristics of the AIO TFT annealed at 350°C for 2 h with various gate voltages. (b) Transfer characteristics of AIO TFTs and indium oxide TFT for $V_{DS} = 40$ V with structure of $L = 220$ μm and $W = 1000$ μm.

resulting channel mobility is $\mu = 19.6$ cm^2/V s with an n-type semiconductor behavior, which is competitive with vacuum-processed oxide TFTs annealed at low temperature. The threshold voltage is ~10 V operating in the accumulation mode on a positive gate bias, the subthreshold swing is 0.3 V/decade, and the on-to-off current ratio is about 1.7×10^8 with an especially low off-current of 8.1×10^{-12} A, as seen in Fig. 3b. The resultant electrical property is superior to the result of solution-based oxide TFTs and even similar to vacuum processes.

Although thermal decomposition was not completed at 300°C, basic TFT performances, such as current saturation and switching behaviors, were observed even at the 300°C annealed case. The summarized electrical properties for both cases, 300 and 350°C, are shown in Table I. The similar subthreshold swing, which gives information on defects in a film, points out that organics are removed well even at the 300°C annealing process. The dramatic improvement in mobility originates from the crystallization of the film. The XRD patterns shown in Fig. 1b indicate that the AIO film annealed at 300°C shows an amorphous phase, whereas a clear peak appears at the 350°C annealed one, which results in a much higher electron conduction property. As a result, it seems reasonable that the crystallization process starts at a certain critical temperature between 300 and 350°C and leads to a much better electrical property for the 350°C annealed case.

Table I. Electrical property of AIO TFTs annealed at various temperatures.

Temperature (°C)	μ_{sat} (cm^2/V s)	I_{on}/I_{off}	V_{th} (V)	S (V/decade)
300[a]	1.1	7.7×10^6	~25	0.4
350	19.6	1.7×10^8	~10	0.3

[a] At a fixed $V_{DS} = 40$ V with a structure of $L = 220$ μm and $W = 1000$ μm.

It was observed that the electrical property of TFTs was improved by substituting Al on In sites in the In_2O_3 lattice specifically in terms of off-current, which originates from the controlling carrier concentration, compared to that of the In_2O_3 TFTs. The incorporation of Al ions, which forms stronger chemical bonds with oxygen than with In, suppresses carrier generation via the formation of oxygen vacancies.[8] Thus, electron conduction is restricted and carrier concentration is lowered under an insufficient electric field that leads to a low off-current at an off-state. Consequently, we were able to fabricate the TFT, which exhibits a low off-current with a high mobility simultaneously.

In conclusion, we have investigated highly transparent multicomposite oxide, AIO, TFTs fabricated via a simple and low cost solution process. Substitution of Al on In sites in the In_2O_3 lattice is verified by a shift in XRD peak and UV/visible absorption spectra. Modification of the lattice structure strongly influences the property of TFTs. They exhibit good electrical property and operate in the accumulation mode on a positive gate bias with SiO_2, which is a commonly used gate dielectric in electrical devices. Their low heat-treatment temperature (350°C) allows for the use of various substrates. These results indicate that solution-processed AIO TFTs are suitable devices for high performance display back-plane and transparent electronics.[1]

Acknowledgments

This research was financially supported by the Ministry of Knowledge Economy (MKE) and the Korea Industrial Technology Foundation (KOTEF) through the Human Resource Training Project for Strategic Technology. This work was also supported by a Korea Science and Engineering Foundation (KOSEF) grant funded by the Korean government (MEST) (grant no. R11-2007-045-03002-0).

Korea Advanced Institute of Science and Technology assisted in meeting the publication costs of this article.

References

1. J. F. Wager, *Science*, **300**, 1245 (2003).
2. H. Hosono, *Thin Solid Films*, **515**, 6000 (2007).
3. V. Subramanian, J. M. J. Frechet, P. C. Channg, D. C. Huang, J. B. Lee, S. E. Molesa, A. R. Murphy, D. R. Redinger, and S. K. Volkman, *Proc. IEEE*, **93**, 1330 (2005).
4. P. Gorrn, M. Sander, J. Meyer, M. Kroger, E. Becker, H. Johannes, W. Kowalsky, and T. Riedl, *Adv. Mater. (Weinheim, Ger.)*, **18**, 738 (2006).
5. R. L. Hoffman, B. J. Norris, and J. F. Wager, *Appl. Phys. Lett.*, **82**, 733 (2003).
6. B. Yaglioglu, H. Y. Yeom, R. Beresford, and D. C. Paine, *Appl. Phys. Lett.*, **89**, 062103 (2006).
7. H. Q. Chiang, J. F. Wager, R. L. Hoffman, J. Jeong, and D. A. Keszler, *Appl. Phys. Lett.*, **86**, 013503 (2005).
8. K. Nomura, H. Ohta, A. Takagi, T. Kamiya, M. Hirano, and H. Hosono, *Nature (London)*, **432**, 488 (2004).
9. L. Wang, M. Yoon, G. Lu, Y. Yang, A. Facchetti, and T. J. Marks, *Nature Mater.*, **5**, 893 (2006).
10. Y. Qijun and L. Dejie, *Phys. Status Solidi A*, **205**, 389 (2008).
11. R. B. H. Tahar, T. Ban, Y. Ohya, and Y. J. Takahashi, *J. Appl. Phys.*, **83**, 2139 (1998).
12. D. Lee, Y. Chang, G. S. Herman, and C. Chang, *Adv. Mater. (Weinheim, Ger.)*, **19**, 843 (2007).
13. B. S. Ong, C. Li, Y. Li, Y. Wu, and R. Loutfy, *J. Am. Chem. Soc.*, **129**, 2750 (2007).
14. S. Seo, C. G. Choi, Y. H. Hwang, and B. Bae, *J. Phys. D: Appl. Phys.*, **42**, 035106 (2009).
15. D. Lee, S. Han, G. S. Herman, and C. Chang, *J. Mater. Chem.*, **19**, 3135 (2009).
16. J. J. Schneider, R. C. Hoffmann, J. Engstler, O. Soffke, W. Jaegermann, A. Issanin, and A. Klyszcz, *Adv. Mater. (Weinheim, Ger.)*, **20**, 3383 (2008).
17. D. Lee, Y. Chang, W. Stickle, and C. Chang, *Electrochem. Solid-State Lett.*, **10**, K51 (2007).
18. C. G. Choi, S. Seo, and B. Bae, *Electrochem. Solid-State Lett.*, **11**, H7 (2008).

19. Y. Chang, D. Lee, G. S. Herman, and C. Chang, *Electrochem. Solid-State Lett.*, **10**, H135 (2007).
20. M. Orita, H. Ohta, M. Hirano, S. Narushima, and H. Hosono, *Philos. Mag. B*, **81**, 501 (2001).
21. H. Hosono, K. Nomura, Y. Ogo, T. Uruga, and T. Kamiya, *J. Non-Cryst. Solids*, **354**, 2796 (2008).
22. H. S. Kim, P. D. Byrne, A. Facchetti, and T. J. Marks, *J. Am. Chem. Soc.*, **130**, 12580 (2008).
23. B. J. Norris, J. Anderson, J. F. Wager, and D. A. Keszler, *J. Phys. D: Appl. Phys.*, **36**, L105 (2003).
24. H. J. Chun, Y. S. Choi, S. Y. Bae, H. C. Choi, and J. Park, *Appl. Phys. Lett.*, **85**, 461 (2004).